First publ. in: Jornal of Physics: Condensed Matter 19 (2007), 205132

Nonequilibrium structure of concentrated colloidal fluids under steady shear: leading-order response

Oliver Henrich, Oskar Pfeifroth and Matthias Fuchs

Department of Physics, University of Konstanz, Universitätsstraße 10, D-78457 Konstanz, Germany

Received 15 December 2006, in final form 3 January 2007
Published 25 April 2007
Online at stacks.iop.org/JPhysCM/19/205132

Abstract
The flow-induced microstructural distortions of dense colloidal dispersions under steady shearing are derived within a recent first-principles approach to the nonlinear rheology of colloidal fluids and glasses. The stationary structure factor is discussed to leading orders in shear rate $\dot\gamma$. We find that shear affects the stationary structure whenever the dressed Peclet/Weissenberg number $Pe = \dot\gamma\tau$ becomes appreciable; here τ is the structural or α-relaxation time. Close to vitrification, this predicts significantly larger shear distortions than expected from considering the bare Peclet number Pe_0; it compares $\dot\gamma$ with the diffusion time of a colloid at infinite dilution.

(Some figures in this article are in colour only in the electronic version)

1. Introduction

Dynamic light scattering [1], rheometry [2], microscopy [3], and Brownian dynamics simulations [4] have revealed that colloidal dispersions undergo a glass transition upon densification. Detailed comparisons of the observed structural (glassy) relaxation with first-principles calculations from mode coupling theory (MCT) [5–7] have shown that many aspects of this transition closely follow the MCT scenario of an idealized glass transition [8].

Dense colloidal dispersions also exhibit quite interesting behaviours under external shear flow, which often have been linked with either flow-induced ordering phenomena, solvent-induced (lubrication) interactions, and/or an approach to random close packing; for a recent review of theoretical approaches see [9]. The viscosity strongly decreases even under small applied steady shear rates (shear thinning) [10], and the microstructure as described by the structure factor or pair correlation function gets distorted [11, 12]. Stationary states not describable by a Gibbs–Boltzmann distribution function can easily be obtained, and sheared dispersions thus present a model system for the study of driven (metastable) states far from equilibrium.

Recently, an extension of MCT to systems under steady shearing was developed that unites the fields of glass transition and rheology [13]. It predicts shear thinning, yielding of colloidal

glasses, a speed up of structural relaxation under shear caused by advection of fluctuations, and a dependence of the microstructure on shear rate. The latter can be expected to provide insights into the microscopic mechanisms of particle rearrangements in fluid and glassy states under strong shear. Specific to the theory is an integration through transients (ITT) approach that enables one to derive stationary expectation values from transient time-dependent structural correlations.

In this contribution, we present first results on the distorted stationary microstructure of Brownian hard-sphere fluids to leading orders in the shear rate. This enables us to compare our approach with previous theories, with experiments and with simulations. We find that all existing microscopic theories severely failed to account for the magnitude of structural deformation under shear at high densities, because the slowing down of the structural relaxation close to the glass transition was not taken into account.

2. Theory

Steady-state properties of sheared dispersions result from a competition between Brownian diffusion and flow with shear rate $\dot\gamma$. Their relative importance can be measured by the bare Peclet number $Pe_0 = \dot\gamma D^2/D_0$, where D_0 is the short-time single-particle diffusion coefficient and D the particle diameter. In the integration through transients (ITT) approach, the competition between diffusion and flow enters into stationary expectation values via generalized Green–Kubo relations that contain the complete transient time evolution of the system. For the steady-state structure factor $S_{\mathbf{q}}^{(\dot\gamma)}$ of density fluctuations under shearing in plain Couette flow ($\mathbf{v} = \dot\gamma y\hat{\mathbf{x}}$, neglecting velocity fluctuations and hence hydrodynamic interactions) we find [13]

$$S_{\mathbf{q}}^{(\dot\gamma)}(\dot\gamma) = \frac{1}{N}\langle\varrho_{\mathbf{q}}^*\varrho_{\mathbf{q}}\rangle + \frac{\dot\gamma}{Nk_{\mathrm{B}}T}\int_0^\infty \mathrm{d}t\,\langle\sigma_{xy}\mathrm{e}^{\Omega^\dagger t}\varrho_{\mathbf{q}}^*\varrho_{\mathbf{q}}\rangle \tag{1}$$

with $S_q = \frac{1}{N}\langle\varrho_{\mathbf{q}}^*\varrho_{\mathbf{q}}\rangle$ the equilibrium structure factor for wavevector $\mathbf{q}$, and N the particle number. Equilibrium averages are indicated by $\langle\cdots\rangle$. Equation (1) is formally exact, and non-perturbative in $\dot\gamma$ because the Smoluchowski operator Ω [14] depends on the shear rate. More details of the general approach can be found in [13, 15]. The above expression is evaluated by means of the Zwanzig–Mori projection operator formalism and by applying a mode-coupling approximation [8]. This encodes the dynamics of the system in terms of transient density correlation functions, which need to be calculated self-consistently. The vertex coupling the quantities in equation (1) to density fluctuations contains[1]

$$V_{\mathbf{k}}^{\varrho_{\mathbf{q}}^*\varrho_{\mathbf{q}}} = \langle\varrho_{\mathbf{k}}^*\varrho_{\mathbf{k}}Q\varrho_{\mathbf{q}}^*\varrho_{\mathbf{q}}\rangle/N = 2NS_q^2\delta_{\mathbf{q}k} - S_0\varrho\left(S_k + \varrho\frac{\partial S_k}{\partial\varrho}\right)\frac{\partial S_q}{\partial\varrho} \tag{2}$$

with $Q = 1 - \sum_{\mathbf{q}'}\varrho_{\mathbf{q}'}\rangle(1/NS_{q'})\langle\varrho_{\mathbf{q}'}^*$, and the average density ϱ. With equation (3) from [13], this finally yields the approximation for the distorted structure factor $S_{\mathbf{q}}^{(\dot\gamma)}$ in the ITT approach:

$$\begin{aligned} S_{\mathbf{q}}^{(\dot\gamma)} = S_q + \dot\gamma\left\{\int_0^\infty \mathrm{d}t\,\frac{q_xq_y(t)}{q(t)}S'_{q(t)}\frac{S_q^2}{S_{q(t)}^2}\Phi_{\mathbf{q}}^2(t)\right\} \\ - \frac{\dot\gamma S_0}{2}\frac{\partial S_q}{\partial\varrho}\left\{\int_0^\infty \mathrm{d}t\int\frac{\mathrm{d}^3k}{(2\pi)^3}\frac{k_xk_y(t)}{k(t)S_{k(t)}^2}S'_{k(t)}\left(S_k + \varrho\frac{\partial S_k}{\partial\varrho}\right)\Phi_{\mathbf{k}}^2(t)\right\}, \end{aligned} \tag{3}$$

[1] The factor 2 in equation (2) arises from Wick's theorem assuming a Gaussian decoupling of the four-point correlation, and from recognizing that only the fluctuating part $\delta\varrho_{\mathbf{q}}^*\varrho_{\mathbf{q}} = \varrho_{\mathbf{q}}^*\varrho_{\mathbf{q}} - \langle\varrho_{\mathbf{q}}^*\varrho_{\mathbf{q}}\rangle$ enters into equation (1). Also, Baxter's result $\lim_{q'\to 0}\langle\varrho_{\mathbf{q}}^*\varrho_{\mathbf{q}}\varrho_{\mathbf{q}'}\rangle/(NS_{q'}) = S_q + \varrho\partial S_q/\partial\varrho$ is used [20], and evaluating the projector Q at $\mathbf{q}' = 0$ we set $\langle\varrho_{\mathbf{q}'}\langle\varrho_{\mathbf{q}}^*\varrho_{\mathbf{q}}\rangle\rangle/\langle\varrho_{\mathbf{q}'}^*\varrho_{\mathbf{q}'}\rangle = S_q$.

where the advected wavevector and its norm are time dependent according to $\mathbf{q}(t) = (q_x, q_y + q_x\dot{\gamma}t, q_z)$ and $q(t) = |\mathbf{q}(t)|$. The abbreviation $S'_q = \frac{\partial S}{\partial q}$ enters. The correlators $\Phi_\mathbf{q}(t) = \langle \varrho^*_{\mathbf{q}(t)} \mathrm{e}^{\Omega^\dagger t} \varrho_\mathbf{q} \rangle / (N S_q)$ are the normalized transient density correlators. They describe the relaxation of density fluctuations whose magnitude is the equilibrium one, whose time dependence, however, is affected by shear flow. We refer to the second and to the third term on the right-hand side of equation (3) as the anisotropic $\delta S_\mathbf{q}^{(\dot{\gamma},\mathrm{aniso})}$ and the isotropic $\delta S_q^{(\dot{\gamma},\mathrm{iso})}$ contribution to $\delta S_\mathbf{q}^{(\dot{\gamma})}$, the deviation between the distorted and equilibrium structure factor. For any shear rate $\dot{\gamma}$, only the isotropic contribution survives in the plane perpendicular to the flow direction, namely for $q_x = 0$. Computation of the distorted structure now requires solution of the equations for $\Phi_\mathbf{q}(t)$ from [13], which is difficult because of the anisotropic structural rearrangements under shear. An expansion of equation (3) for small shear rates circumvents this problem and gives the leading-order results for the distorted microstructure. It requires only known (isotropic) equilibrium density correlators $\Phi_q(t)$ from standard MCT. The expansion gives the anisotropic part in linear order and the isotropic one in quadratic order in $\dot{\gamma}$:[2]

$$S_q^{(\dot{\gamma})} = S_q + \dot{\gamma}\left\{\frac{q_x q_y}{q} S'_q \int_0^\infty \mathrm{d}t\, \Phi_q^2(t)\right\} + \mathcal{O}(\dot{\gamma}^2 q_x q_y, \dot{\gamma}^2 q_x^2) + \mathcal{O}(\dot{\gamma}^3) - \dot{\gamma}^2 \frac{S_0}{2}\frac{\partial S_q}{\partial \varrho} \times \left\{\int \mathrm{d}k\, \frac{k^3}{6\pi^2}\left(\frac{S'_k}{S_k^2} - \frac{k^2}{5}\partial_k\left(\frac{S'_k}{k S_k^2}\right)\right)\left(S_k + \varrho\frac{\partial S_k}{\partial \varrho}\right)\int_0^\infty \mathrm{d}t\, t\Phi_k^2(t)\right\}. \quad (4)$$

Given the density and the equilibrium S_q, which also determine the quiescent MCT equations used for calculating $\Phi_q(t)$, the distorted microstructure is obtained from equation (4) for small shear rates. Note that to this order in $\dot{\gamma}$ the expansion coefficients are well defined [9]. Equation (3) indicates that the (dressed) Peclet/Weissenberg number Pe, with $Pe = \dot{\gamma}\tau$, is the small parameter in the present expansion; here τ is the final (α-) relaxation time which becomes arbitrarily large at the glass transition. The range of usefulness of equation (4) thus shrinks rapidly when approaching vitrification. Yet, because the distortion in linear order has been the topic of a number of theoretical approaches (see [11, 16, 17] and references therein), a numerical evaluation of equation (4) appears useful.

3. Results

The numerical solutions to the quiescent MCT equations have been calculated using well-established algorithms [18]. We used a similar discretization like [19] but with a refined q-grid of 400 wavevectors, a spacing of $qD = 0.1$ and a cutoff of $qD = 40$. Throughout the analysis a hard-sphere structure factor with a Percus–Yevick closure was used with a critical packing fraction of $\phi_\mathrm{c} = (\pi/6)\varrho_\mathrm{c} D^3 = 0.516$ [8]. The critical packing fractions used for experiment and Brownian dynamics simulation are $\phi_\mathrm{c} = 0.58$.

Figure 1 shows the normalized anisotropic contribution $\delta S_\mathbf{q}^{(\dot{\gamma},\mathrm{aniso})}$ to the distorted structure factor for packing fractions $\phi = 0.36, 0.44$ and 0.46. Data taken from Brownian dynamics simulations at $\phi = 0.43$ and 0.5 from [11] are also included. In both cases the data were divided by a factor $\dot{\gamma} q_x q_y / q^2$, which is the origin of the trivial anisotropy in the leading linear order. The distortion $\delta S_\mathbf{q}^{(\dot{\gamma},\mathrm{aniso})}$ of the microstructure grows strongly with ϕ, because of the approach to the glass transition. The $\delta S_\mathbf{q}^{(\dot{\gamma},\mathrm{aniso})}$ is proportional to the α-relaxation time τ, as proven in the left inset of figure 1. Here, τ is estimated from $\Phi_{q_p}(t = \tau) = 0.1$, where q_p

[2] A small correction arising from anisotropies in $\Phi_\mathbf{q}(t)$ is neglected in the isotropic term.

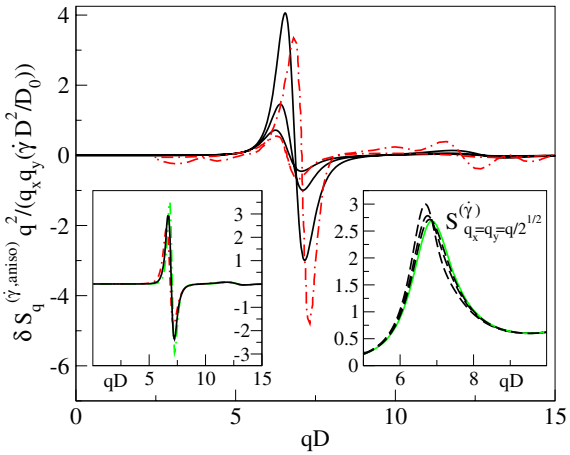

Figure 1. Anisotropic contribution to $\delta S_{\mathbf{q}}^{(\dot\gamma,\mathrm{aniso})}$ in leading order normalized to $\dot\gamma q_x q_y/q^2$ (black solid lines). Decreasing the relative separations from the critical point as $\varepsilon = -0.2, -0.15, -0.1$, the magnitude of $\delta S_{\mathbf{q}}^{(\dot\gamma)}$ increases. The dashed–dotted red curves are Brownian dynamics simulation data from [11] using the same normalization at $\varepsilon = -0.259, -0.138$. The right inset shows the unnormalized $S_{\mathbf{q}}^{(\dot\gamma)}$ along the extensional axis $q_x = q_y = q/\sqrt{2}$ at $\varepsilon = -0.1$ and, from bottom to top, $Pe = \dot\gamma\tau = 0$ (green—solid), 1/8, 1/4 and 1/2 (all black—dashed), where $\Phi_{q_p}(t=\tau) = 0.1$ defines τ. $Pe/Pe_0 = 1.66$ holds at this ε. The left inset shows the data of the main figure rescaled with the dressed Peclet number, $\delta S_{\mathbf{q}}^{(\dot\gamma,\mathrm{aniso})}/(Pe\, q_x q_y/q^2)$; for $\varepsilon = -0.1, -0.05$, and -0.01 (with increasing peak height) the values $Pe/Pe_0 = 1.66$, $Pe/Pe_0 = 8.06$, and $Pe/Pe_0 = 419$ are used.

denotes the position of the primary peak in S_q. The strongest shear dependence occurs for the direction of the extensional component of the flow, $q_x = q_y$. Here, the mesoscale order of the dispersion grows; the peak in $\delta S_{\mathbf{q}}^{(\dot\gamma,\mathrm{aniso})}$ increases and sharpens. While the theoretical $\delta S_{\mathbf{q}}^{(\dot\gamma,\mathrm{aniso})}$ turns out rather symmetric around the peak of the quiescent structure factor ($q_p D \approx 7.0$), the simulations exhibit a deeper negative dip at $q > q_p$. Its origin is unclear, but it may arise in part from small differences in the quiescent S_q used here and in [11] which are enlarged by the derivative S_q' in equation (4). The simulations were actually not performed for a hard-sphere system but rather for a screened Coulomb system and then mapped onto effective hard-sphere volume fractions by comparing the resulting structure factors.

Figure 2 depicts the distorted structure factor $S_{\mathbf{q}}^{(\dot\gamma)}$ in the plane perpendicular to the flow, namely for $q_x = 0$. There, only the isotropic term $\delta S_q^{(\dot\gamma,\mathrm{iso})}$ contributes to leading quadratic order in shear rate. The structure factor is somewhat decreased around the peak. Presumably, because of the minute magnitude of this quadratic effect, experimental data have been obtained only at higher Peclet numbers, where the shear dependence of the structural relaxation cannot be neglected any longer. The neutron scattering measurements of [12] scale like $\dot\gamma^x$ with an exponent $1/4 \leqslant x \leqslant 3/4$ instead of 2. Nevertheless, the data are included in figure 2 in order to test the qualitative contents of our results. The quadratic theoretical expression was extrapolated beyond its limit of validity to the bare Peclet number $Pe_0 = 1/2$, whereas the experimental data correspond to shear rates $Pe_0 = 1.64$–4.8 in the shear-thinning regime. While the theories discussed in [11, 16] predict no change of the microstructure for $q_x = 0$, our results rationalize the experimental observations and are consistent with exact solutions in the low-density limit [17].

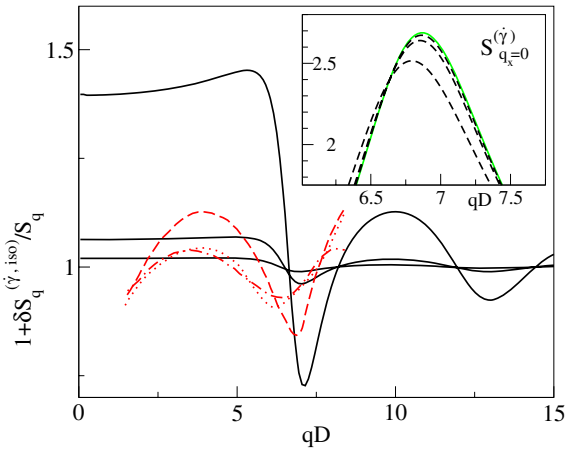

Figure 2. Normalized structure factor $S_{\mathbf{q}}^{(\dot\gamma)}/S_q$ in the plane perpendicular to the flow direction, $q_x = 0$. It is given by $1 + \delta S_q^{(\dot\gamma,\mathrm{iso})}/S_q$ in leading quadratic order, and is calculated for $Pe_0 = 1/2$ (black solid lines). The separation parameters are from bottom to top $\varepsilon = -0.2, -0.15, -0.1$. Red lines are experimental data taken from [12] at $\varepsilon = -0.207$ (dashed–dotted), -0.155 (dotted), -0.103 (long-dashed) and $Pe_0 = 1.64, 2.88, 4.8$, respectively; all Peclet numbers lie outside the expected range of validity of equation (4). The inset shows the unnormalized $S^{(\dot\gamma)}_{q_x=0}$ at $\varepsilon = -0.1$ and, from top to bottom, $Pe = \dot\gamma\tau = 0$ (green—solid), 1/8, 1/4 and 1/2 (all black—dashed), where $\Phi_{q_p}(t = \tau) = 0.1$ defines τ. $Pe/Pe_0 = 1.66$ at this ε.

4. Discussion

The stationary structural correlations of a dense fluid of spherical particles undergoing Brownian motion, neglecting hydrodynamic interactions, change with shear rate $\dot\gamma$ in response to a steady shear flow. In linear order, the structure is distorted only in the plane of the flow, while already in second order in $\dot\gamma$, the structure factor changes under shear also for wavevectors lying in the plane perpendicular to the flow. Consistent with previous theories, we find regular expansion coefficients in linear and quadratic order in $\dot\gamma$ for fluid (ergodic) suspensions. While previous microscopic theories developed for higher densities predicted no change of the microstructure for $q_x = 0$ [11, 16], our approach does, which is in qualitative agreement with experiments [12].

Our most important finding concerns the magnitude of the distortion of the microstructure, and the dimensionless parameter measuring the effect of shear relative to the intrinsic particle motion. This topic can already be discussed using the linear-order result, and is not affected by considerations of hydrodynamic interactions, as can be seen from comparing Brownian dynamics simulations [11] and experiments on dissolved particles [12]. In previous theories, shear rate effects enter when the bare Peclet number Pe_0 becomes non-negligible. In the present ITT approach the dressed Peclet/Weissenberg number $Pe = \dot\gamma\tau$ governs the shear effects; here, τ is the (final) structural relaxation time. Shear flow competes with structural rearrangements that become arbitrarily slow compared to diffusion of dilute particles when approaching the glass transition. The distorted microstructure results from the competition between shear flow and cooperative structural rearrangements. It is thus no surprise that previous theories using Pe_0, which is characteristic for dilute fluids or strong flows, had severely underestimated the magnitude of shear distortions in hard-sphere suspensions for higher packing fractions; references [11, 16] report an underestimate by roughly a decade at $\phi = 0.50$. The ITT approach actually predicts a divergence of $\lim_{\dot\gamma\to 0}(S_{\mathbf{q}}^{(\dot\gamma)} - S_q)/\dot\gamma$ for density approaching the

glass transition at $\phi_c \approx 0.58$. We believe that the reassuring agreement of ITT results on $S_{\mathbf{q}}^{(\dot{\gamma})}$ with data from simulations show that in the ITT approach the correct expansion parameter Pe has been identified. We see this as support for the strategy introduced in [13] to connect the nonlinear rheology of dense dispersions with the structural relaxation studied at the glass transition.

Acknowledgment

OH was supported by the International Research Training Group 'Soft Condensed Matter' of the Deutsche Forschungsgemeinschaft (DFG).

References

[1] van Megen W and Underwood S M 1993 *Phys. Rev. Lett.* **70** 2766
van Megen W and Underwood S M 1994 *Phys. Rev.* E **49** 4206
Eckert T and Bartsch E 2003 *Faraday Discuss.* **123** 51
[2] Mason T G and Weitz D A 1995 *Phys. Rev. Lett.* **75** 2770
Petekidis G, Vlassopoulos D and Pusey P N 2003 *Faraday Discuss.* **123** 287
Petekidis G, Moussaid A and Pusey P N 2002 *Phys. Rev.* E **66** 051402
[3] Weeks E R, Crocker J C, Levitt A C, Schofield A and Weitz D A 2000 *Science* **287** 627
[4] Flenner E and Szamel G 2005 *Phys. Rev.* E **72** 011205
[5] Götze W 1999 *J. Phys.: Condens. Matter* **11** A1
[6] Sperl M 2005 *Phys. Rev.* E **71** 060401
[7] Voigtmann T, Puertas A M and Fuchs M 2004 *Phys. Rev.* E **70** 061506
[8] Götze W 1991 *Liquids, Freezing and Glass Transition* ed J-P Hansen, D Levesque and J Zinn-Justin (Amsterdam: North-Holland) p 287
[9] Bergenholtz J 2001 *Curr. Opin. Colloid Interface Sci.* **6** 484–8
[10] Petekidis G, Vlassopoulos D and Pusey P N 2004 *J. Phys.: Condens. Matter* **16** S3955
Crassous J, Siebenbürger M, Ballauff M, Drechsler M, Henrich O and Fuchs M 2006 *J. Chem. Phys.* **125** 204906
[11] Szamel G 2001 *J. Chem. Phys.* **114** 8708
[12] Johnson S J, de Kruif C G and May R P 1988 *J. Chem. Phys.* **89** 5909
[13] Fuchs M and Cates M E 2002 *Phys. Rev. Lett.* **89** 248304
[14] Dhont K J G 1996 *An Introduction to the Dynamics of Colloids* (Amsterdam: Elsevier)
[15] Fuchs M and Cates M E 2005 *J. Phys.: Condens. Matter* **17** 1681
[16] Lionberger R A and Russel W B 2000 *Adv. Chem. Phys.* **111** 399
[17] Blawzdziewicz J and Szamel G 1993 *Phys. Rev.* E **48** 4632
[18] Fuchs M, Götze W, Hofacker I and Latz A 1991 *J. Phys.: Condens. Matter* **3** 5047
[19] Franosch T, Fuchs M, Götze W, Mayr M R and Singh A P 1997 *Phys. Rev.* E **55** 7153
[20] Baxter R J 1964 *J. Chem. Phys.* **41** 553